Kinetic Study on Methanol Dehydration to Dimethyl Ether Applying Clinoptilolite Zeolite as the Reaction Catalyst

Maryam Kasaie[1] and Morteza Sohrabi [2*]

[1] Chemical Engineering Department, Amirkabir University of Technology, Hafez Avenue, Tehran 15914, Iran
[2] Chemical Engineering Department, Amirkabir University of Technology, Hafez Avenue, Tehran 15914, Iran and Iran Academy of Sciences, Darband Street, Tehran 19717, Iran, sohrabi@aut.ac.ir, Tel. (+98)21 64543155, Fax. (+98)2166405847.

Abstract. Dehydration of methanol to dimethyl ether (DME), using clinoptilolite-zeolite as the reaction catalyst, within the temperature range of 300-350 °C has been studied in a continuous fluidized bed reactor. The reactor was a cylindrical tube, 26 mm internal diameter and 0.5 m high, placed vertically in a furnace. The effects of some pertinent operating parameters, such as temperature, superficial gas velocity, catalyst's particle size, and methanol partial pressure, on the extent of dehydration reaction have been investigated. Two hydrodynamic models presented for bubbling fluidized bed reactors, i.e., Kunii - Levenspiel (K-L) as an example of three phase models and El-Halwagi - El-Rifai (H-R) as an example of compartment models were applied to correlate the experimental data. It was determined that the mean absolute deviation between the experimental data and those predicted from K-L model was lower than that observed in the case of H-R model (19% and 70%, respectively). Among the operating parameters, partial pressure of methanol was found to have the highest impact on the process yield.
Key words: Methanol, Dimethyl ether; Clinoptilolite, Bubbling fluidized bed reactor, Kinetic model.

Resumen. Se describe un studio de la deshidratación de metanol que conduce a la formación del éter dimetílico (EDM) mediante catálisis con clinoptilolita-zeolita, dentro del intervalo de temperatura de 300-350 ºC, en un reactor de cama fluidizada. Este último consistió en un tubo cilíndrico, de 26 cm de diámetro interno y 50 cm de alto, que fue colocado verticalmente en un horno. También se investigaron los efectos de algunos parámetros, tales como la temperatura, la velocidad del gas superficial, el tamaño de partícula del catalizador y la presión parcial del metanol, sobre el avance de la reacción de deshidratación. Se aplicaron dos modelos hidrodinámicos sobre el burbujeo en el reactor de cama fluidizada, con el fin de correlacionar los datos experimentales: (a) el modelo de Kunii - Levenspiel (K-L), como ejemplo de modelos de tres fases; y (b) el modelo de El-Halwagi - El-Rifai (H-R), como un ejemplo de modelo de compartimento. Se determinó que la desviación absoluta media entre los datos experimentales y aquellos predichos por el modelo K-L fue más baja que aquella observada mediante el modelo H-R (19% y 70%, respectivamente). Se encontró que, entre los parámetros de operación, la presión parcial del metanol tuvo el mayor impacto sobre la eficiencia del proceso.
Palabras clave: Metanol, éter dimetílico, clinoptilolita, reactor cama fluidizada por burbujeo, modelo cinético.

Introduction

Dimethyl ether is a multi-purpose clean energy carrier for the 21st century obtained from chemical conversion of natural gas or coal. DME is non-toxic and is currently used as aerosol propellants and refrigerant as a substitute for chlorofluorocarbons. The property of DME is very attractive as a substitute for LPG and diesel oil and as a clean fuel without SO_x and soot emission. DME can be handled similarly as LP Gas and is condensed at -25 °C under atmospheric pressure or at a pressure of 5 to 6 bar at ambient temperature. Existing tankers and receiving terminals of LP Gas can be easily converted to those for DME distribution. DME can be manufactured using either of the following two processes: direct conversion of synthesis gas or methanol dehydration (MTD).

At present, DME is commercially prepared by MTD process applying acidic porous catalysts including Zeolites, silica–alumina and alumina. DME synthesis from synthesis gas is currently under development in research institutes. [1-4]

Methanol dehydration reaction is presented by the following relation,

$$2CH_3OH \rightleftharpoons CH_3OCH_3 + H_2O \qquad \Delta H_r = -21.555\,kJ/mol \quad (1)$$

Fluidized bed reactors may be regarded as ideal systems for DME synthesis. Compared with fixed-bed reactor, the gas–solid mass transfer resistance in a fluidized bed reactor could be neglected and excellent temperature control is achievable due to the vigorous mixing of catalyst particles in the bed. In the present study the performance of a fluidized-bed reactor for DME synthesis has been evaluated applying Kunii-Levenspiel and El-Halwagi models. In addition, the effects of several pertinent parameters such as particle size, temperature, methanol partial pressure and superficial gas velocity on conversion and yield of methanol have been investigated.
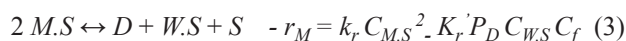
Results and discussion

Kinetic model

Eley-Ridel and Langmuir–Hinshelwood mechanisms have been proposed for a number of catalytic dehydration reactions [5-11]. In the present study the Langmuir–Hinshelwood formulation was considered for dehydration of methanol. According to such a mechanism the following steps may be assumed:

$$M + S \leftrightarrow M.S \qquad K_M P_M C_f = C_{M \cdot S} \qquad (2)$$
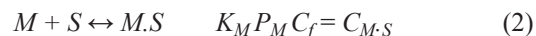
Table 1. Predicted values for parameters of equation (6)

Temperature (°C)	K'_r (g mol)(min)$^{-1}$(g catalyst)$^{-1}$(bar)$^{-1}$	K_W (bar)$^{-1}$	K_M (bar)$^{-1}$	k_r (g mol)(min)$^{-1}$(g catalyst)$^{-1}$	R_{sqr}
0.9523	9E-9	4.07E-7	21.28	1.666E-4	310
0.934	1.041E-8	1.591E-7	11.121	3.011E-4	330
0.933	3.671E-8	7.462E-8	9.956	3.727E-4	350

$$2\,M.S \leftrightarrow D + W.S + S \quad -r_M = k_r C_{M.S}{}^2 - K_r' P_D C_{W.S} C_f \quad (3)$$

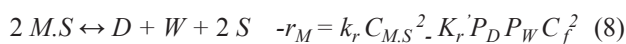$$W + S \leftrightarrow W.S \quad K_W P_W C_f = C_{W.S} \quad (4)$$

Where,

$$C_t = C_f + C_{M.S} + C_{W.S} \quad C_t = C_f(1 + K_M P_M + K_W P_W) \quad (5)$$

The final relation is obtained as follows,

$$-r_M = \frac{k_r K_M{}^2 P_M{}^2 - k_r' K_W P_D P_W}{(1 + K_M P_M + K_W P_W)^2} \quad (6)$$

Where *M*, is methanol in the gas phase; *M.S* is an active intermediate consisting of the unique zeolite surface species bounded with the adsorbed methanol; *W* is water; *D* is dimethylether in gas phase and *W.S*, represents adsorbed water on free catalyst acidic sites.

With regard to the data presented in Table1, it is evident that the values for equilibrium constants of water absorption are low. This may indicate that in the reaction temperature, water is rapidly released from the zeolite acidic sites. Thus, the reaction mechanism may be simplified as follows,

$$M + S \leftrightarrow M.S \quad K_M P_M C_f = C_{M.S} \quad (7)$$

$$2\,M.S \leftrightarrow D + W + 2\,S \quad -r_M = k_r C_{M.S}{}^2 - K_r' P_D P_W C_f^2 \quad (8)$$

$$C_t = C_f + C_{M.S} \quad C_t = C_f(1 + K_M P_M) \quad (9)$$

Hence, the rate expression takes the following form,

$$-r_M = \frac{k_r K_M{}^2 P_M{}^2}{(1 + K_M P_M)^2} \quad (10)$$

Based upon the data presented in Table 2, the activation energy for the forward reaction of equation (8) has been determined as 60.12 kJ mole^{-1}.

Design of experiments

In order to study the significance of the process operating parameters and compare the response of each on the system

Table 2. Predicted values for parameters of equation (10)

Temperature (°C)	k_r (g mol)(min)$^{-1}$(g catalyst)$^{-1}$	K_M (bar)$^{-1}$	R_{sqr}
0.9548	21.275	1.666E-4	310
0.9383	11.231	3.024E-4	330
0.9391	9.954	3.723E-4	350

target, selected as DME yield, and to optimize the latter parameters values, an L9 ANOVA table was prepared according to Taguchi experimental design method. In such an analysis 4 factors with 3 levels were selected. Particle size and superficial gas velocity both have strong impacts mainly on hydrodynamic behavior of fluidized bed systems. Whereas, temperature and methanol partial pressure, affect both hydrodynamic of the system and the reaction kinetic. The operating parameters for the reaction systems determined from Taguchi method and the results are summarized in Table 3.
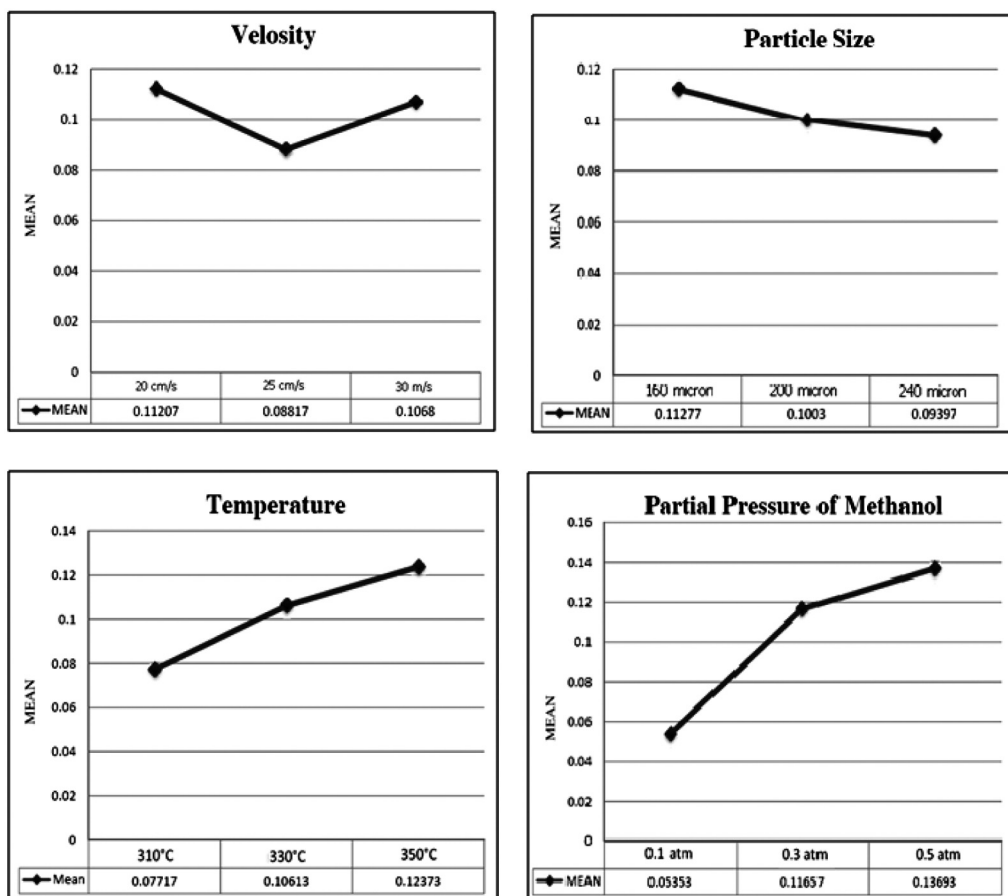
As it may be observed from the above table, the values given for dimensionless diameter (d_p^*) and dimensionless velocity (U^*) correspond exactly to the conditions prevailed within the bubbling fluidized bed systems [12]. Therefore, the bubbling fluidized bed hydrodynamic models may be applied to correlate the present experimental data.

Difference between system response in minimum and maximum levels of each parameter is shown in Figure 1a. In Figure 1b, the relative impacts of operating parameters on the target function is presented. As it may be observed from these
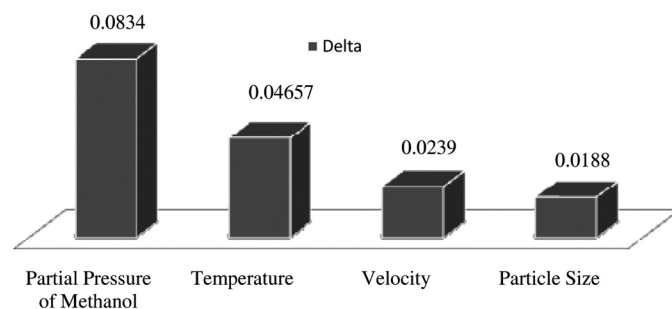
Fig. 1a. Difference between system responses to minimum and maximum levels of each parameter.

Table 3. Operating parameters as determined by Taguchi method and the experimental results

Experiment No.	Particle size (μm)	T (°C)	Partial pressure of methanol (bar)	Superficial gas velocity (cm/s)	U_{mf} (cm/s)	d_p^* (-)	U^* (-)	Conversion (%)	Yield (-)	Methanol Flow rate (cm³/h)	WHSV (lit) / (kg) (h)	Catalyst Activity (g DME) / (g catalyst)(h)
0.0047	1.01	30	0.0485	7.87	0.19	3.66	0.87	20	0.1	310	160	1
0.0272	4.03	120	0.1166	5.25	0.19	3.66	0.87	25	0.3	330	160	2
0.0598	7.66	230	0.1732	4.02	0.19	3.66	0.87	30	0.5	350	160	3
0.0173	5.02	150	0.0938	3.35	0.19	3.66	0.87	30	0.3	310	200	4
0.0439	5.33	160	0.1484	4.99	0.19	3.66	0.87	20	0.5	330	200	5
0.0069	1.33	40	0.0587	8.20	0.19	3.66	0.87	25	0.1	350	200	6
0.0173	6.67	200	0.0892	2.53	0.19	3.66	0.87	25	0.5	310	240	7
0.0061	1.67	50	0.0534	6.40	0.19	3.66	0.87	30	0.1	330	240	8
0.0387	3.01	90	0.1393	8.10	0.19	3.66	0.87	20	0.3	350	240	9

Velocity

	20 cm/s	25 cm/s	30 m/s
MEAN	0.11207	0.08817	0.1068

Particle Size

	160 micron	200 micron	240 micron
MEAN	0.11277	0.1003	0.09397

Temperature

	310°C	330°C	350°C
Mean	0.07717	0.10613	0.12373

Partial Pressure of Methanol

	0.1 atm	0.3 atm	0.5 atm
MEAN	0.05353	0.11657	0.13693

Fig. 1b. Effects of factors' levels on the target function (DME yield)

figures, the order of parameter's influence on the target function is as follows:

1) Partial pressure of methanol
2) Temperature
3) Velocity
4) Particle size

The results from Taguchi analysis showed that the optimum process conditions are:

Table 4. Optimum operating parameters

DME Yield	Conversion (%)	Particle Size (μm)	Superficial Gas Velocity (cm/s)	Partial Pressure of Methanol (bar)	Temperature (°C)
0.197	6.9	160	20	0.5	350

Fig. 2. Comparison between the experimental and predicted data

Temperature = 350 °C; Partial pressure of methanol = 0.5 bar, Inlet velocity of gas = 20 cm/s and the mean particle size of catalyst = 160 μm.

The results of an experimental run, applying optimum process conditions, are shown in table 4.

Correlation of data

The experimental data were correlated with two models selected from two major classes of models presented for bubbling fluidized bed systems, i.e., three phase and compartment models. Kunii-Levenspiel (K-L) [12, 13] as an example of three phase models and El-Halwagi - El-Rifai (H-R) [14] as an example of compartment models were applied.
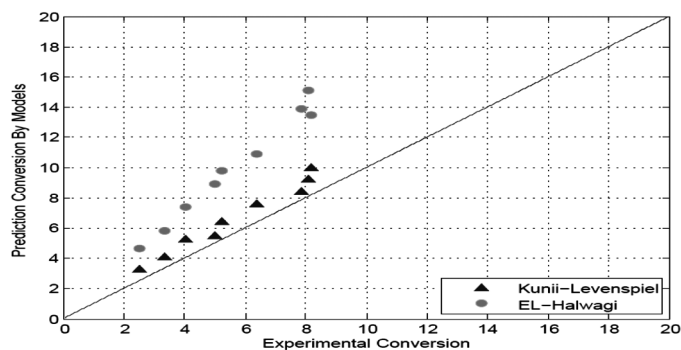
The Kunii-Levenspiel three-phase model may be regarded as a simple but remarkable hydrodynamic model. This model is based upon the following assumptions:

a) Bubbles are of single size and evenly distributed in the bed.
b) Flow of gas in the vicinity of rising bubbles follows the Davidson model.
c) The emulsion phase stays at the minimum fluidization conditions.

The El-Halwagi - El-Rifai model (H-R) is a multi compartment type in which the fluidized bed is divided into a series of similar stages; the height of each is equal to the average equivalent bubble diameter. Further assumptions made are as follows:

a) Each compartment consists of bubble, cloud-wake and emulsion phases.
b) The gas flow rate through the emulsion phase remains at the minimum fluidizing conditions.
c) The flow of emulsion gas is completely mixed within each stage.
d) The bubble phase consists of solid-free bubbles and the gas flowing through the bubble phase is in plug flow.

In Figure 2, a comparison has been made between the experimental results and those predicted from the two models. The mean absolute deviations between the experimental and estimated data from K-L and H-R models are 19% and 70%, respectively.

A possible reason for such discrepancies may be the fact that studies on the behavior of fluidized bed reactors have all been conducted in the absence of chemical reactions. However, the occurrence of chemical reactions in fluidized bed units undoubtedly has certain effects upon the mass transfer rates between the phases and the bubble size distribution within the bed. In addition, the models parameters have all been correlated with certain physical quantities of the system without considering the factors related to the reactions. Another reason may be the complex behavior of the fluidized bed systems that could not be fully described by some fairly simple mathematical relations.

Conclusion

The rate of DME synthesis is affected by the change in temperature and pressure of the system; the entering feed gas velocity and catalyst's particle size. The optimum operating temperature was observed to be 350 °C. Increase in temperature beyond this level may promote the rate of side reactions and enhances the chance of sintering the catalysts particles. Increase in methanol partial pressure has a positive effect on DME production. This is expected with regard to the reaction mechanism and the kinetic model presented. Enhancing the gas velocity has an adverse effect on the extent of reaction which could be explained by the decrease in residence time of reactants within the reactor.

The present investigation could indicate the applicability of fluidized bed reactors in DME synthesis. In addition, a number of advantages of fluidized bed over fixed bed reactors such as the possibility of precise temperature control and absence of external and pore diffusions in catalysts particles could make such units as a prominent substitute for conventional reactors.

A three phase model (K-L) and a compartment model (El-Halwagi) were applied to correlate the experimental results. A comparison between the predicted and experimental data revealed that K-L model seems to be a better representative for the present process.

Experimental

Catalyst preparation

The catalyst applied in this reaction was the treated Iranian natural zeolite (clinoptilolite). This compound has an HEU structure with a Si/Al ratio of 5.78 and an inorganic binder (less than 10 wt %) consists mainly of quartz and cristobalite In order to transform the raw zeolite into the appropriate catalyst, the latter was crushed and divided into three mesh sizes (160, 200 and 240μm). The particles were ion-exchanged with 2N ammonium chloride solution (MERCK) for 24 h under vigorous stirring at room temperature. The resultant mixture was then filtered and the wet powders were washed with hot distilled water. The whole process was repeated twice. The powders were first dried overnight at 100 ºC and then calcined at 500 ºC for 3 h and was used as the catalyst in dehydration reaction.

Catalyst characterization

FTIR spectra of the raw zeolite and the prepared catalyst are given in figures 3a and b. It may be observed that the raw zeolite exhibits an adsorption band in a region close to 3623 cm^{-1}. The bands within the range of 3600-3650 cm^{-1} are normally attributed to the free bridging hydroxyls or Bronsted acid sites. It seems, therefore, that the raw zeolite might have ''intrinsic'' catalytic activity. An interesting point is the attenuation of the band region stated above upon ion exchange with ammonium chloride and subsequent calcination (Fig 1b). Such an observation may be attributed to the transformation of Bronsted acid sites to those of Lewis as the result of dehydration reaction at 500 ºC. Disappearance of bands at wave numbers beyond 3625 cm^{-1} may be related to condensation reactions occurred among different hydroxyl groups during calcination at 500 ºC.

Assessment of catalyst acidity was performed using ammonium temperature programmed desorption (TPD). For this purpose, 0.2 g of catalyst was treated according to the following steps,

a. Purging with helium gas at a flow rate of 30 cm^3/min with simultaneous heating, applying a ramp rate of 10 ºC/min up to 430 ºC with a dwelling time of 180 min.
b. Isothermal adsorption of NH_3 at 100 ºC using a purge gas flow rate of 40 cm^3/min with subsequent dwelling time of 90 min.
c. Desorption of NH_3, applying helium as the carrier gas at a flow rate of 10 cm^3/min with a ramp rate of 10 ºC up to 650 ºC followed by a dwelling period of 20 min.

The apparatus was a TPD/TPT Micrometrics. The thermal conductivity detector was used.

The TPD diagram of the catalyst is shown in Fig. 4. As it is apparent from this figure, the resulting spectrum has a distinct maximum desorption point below 200 ºC followed by a decaying tail extending to approximately 600 ºC. The
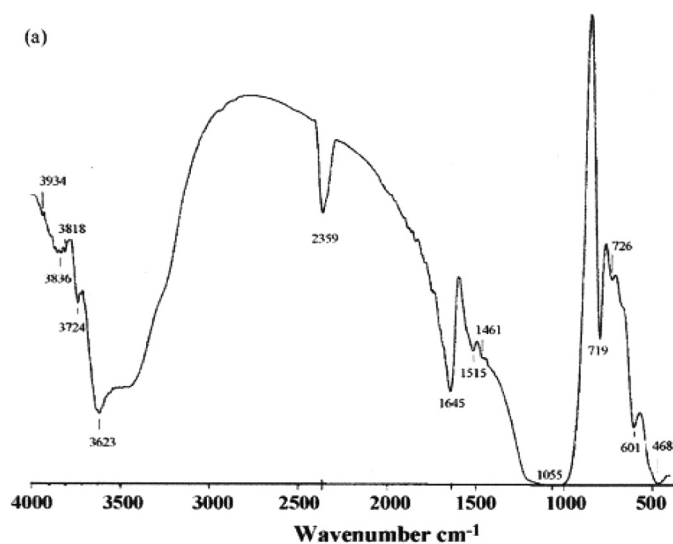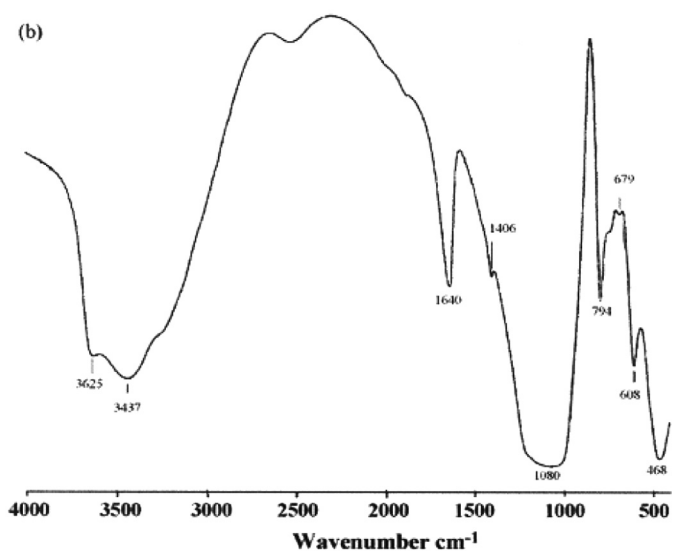

Fig. 3a. FTIR spectrum of the raw zeolite

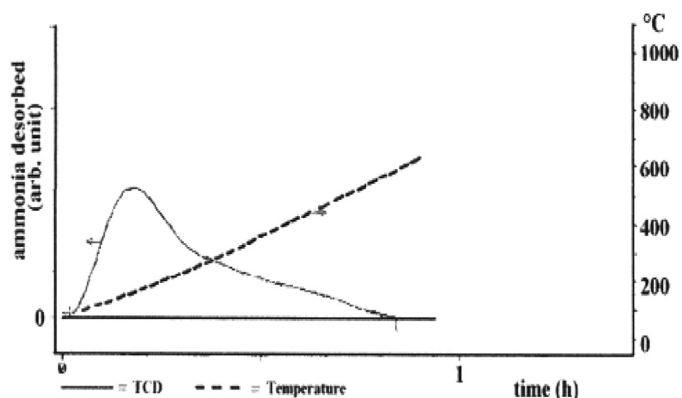**Fig. 3b.** FTIR spectrum of the catalyst

Fig. 4. TPD diagram of the catalyst

total desorption volume was 0.489 cm^3 corresponding to 0.1 mmol of (NH_3)/ (g catalyst). However, it is generally accepted that with NH_3 – TPD or pyridine – TPD analysis, it is not possible to distinguish between Bronsted and Lewis acid sites. Therefore, the FTIR spectrum of the pyridine chemisorbed catalyst was applied to determine the ratio of Bronsted acid sites concentration to that of Lewis acid sites. For both fresh and used catalyst samples the peak area at 1540 cm^{-1} (Bronsted acid sites) was found to be approximately two-fold of that at 1465 cm^{-1} (Lewis acid sites). In addition, no appreciable change in the absolute peak areas was observed with the two samples. Using the extinction coefficients of 3.60 and 2.05 (cm)/μmol for Bronsted and Lewis acid sites, respectively, the corresponding concentrations were calculated as 0.301 and 0.629 (mmol)/g, respectively.

For the fresh catalyst with average particle size of 200 μm, the BET area was 61.463 m^2/g; the total pore volume was 0.0929 cm^3/g and the average pore diameter was 60.503 Å. While, in case of raw zeolite particles with average size of 200 μm, the BET area was 24.00 m^2/g; the total pore volume was 0.0341 cm^3/g and the average pore diameter was 56.789 Å.

Further information concerning this catalyst may be found elsewhere [5, 6].

Start-up procedure

The fluidized-bed reactor applied in the present study consisted of a stainless steel cylindrical tube with 0.026m in diameter and 0.5m high, connected at the top to a truncated cone shaped cyclone separator. The schematic diagram of the experimental rig is shown in Figure 5. In the feed section, the

reactant (methanol) and the carrier gas (N_2) after warming up to the reaction temperature by application of a pre-heater and a furnace were mixed together and was fed to the fluidized-bed reactor via a gas distributor. The reactor contained 30g of catalyst. The temperature was measured by means of a thermocouple housed in the bed. The catalyst was initially placed on the sparger, with a depth of 10-15 cm. The reactant gas mixed with nitrogen entered the reactor at the proper flow rate and velocity via the sparger. When bubbling fluidized conditions were established and stabilized within the bed, usually after ten mean residence times of the bubble phase, a part of the exit gas was conducted to an on-line gas chromatograph apparatus (Agilent model 6890N). The analyzer was equipped with a 0.53 mm×30 m HP-Plot Q capillary column. The TC detector was applied and helium was used as the carrier gas.

References

1. Ogawa, T.; Inoue, I.; Shikada, T.; Ohno, Y. *J. Natural Gas Chem.* **2003**, *12*, 219-227
2. Yaripour, F.; Baghaei, F.; Schmidt, I.; Perregaard, J. *J Catal. Commun.* **2005**, *6*, 147–152
3. Sea, B.; Lee, K-Ho. *Desalination* **2006**, *200*, 689–691
4. Fu, Y.; Hong, T.; Chen, J.; Auroux, A.; Shen, J. *Thermochimica Acta* **2005**, *434*, 22–26
5. Royaee, S. J.; Falamaki, C.; Sohrabi, M.; Talesh, S. S. A. *App. Catal. A: General* **2008**, *338* , 114–120
6. Royaee, S. J.; Sohrabi, M.; Falamaki, C. *Mater. Sci. Poland* **2007**, *25*, 1149–1160
7. Bercic, G.; Levec, J. *Ind. Eng. Chem. Res.* **1992**, *31*, 1035–1040
8. Bercic, G.; Levec, J. *Ind. Eng. Chem. Res.* **1993**, *32*, 2478–2484
9. Gates, B. C.; Johnson, L. N. *AIChE J.* **1971**, *17*, 98–100
10. Blaszkowski, S. R.; van Santen, R.A. *J. Phys. Chem. B* **1997**, *101*, 2292-2305
11. Bandiera, J.; Naccache, C. *Appl. Catal.* **1991**, *69*, 139–148
12. Kunii, D.; Levenspiel, O., *Fluidization Engineering, 2nd Edition.* Butterworth, Boston, **1991**.
13. Levenspiel, O. *Powder Technology* **2002**, *122*, 1–9
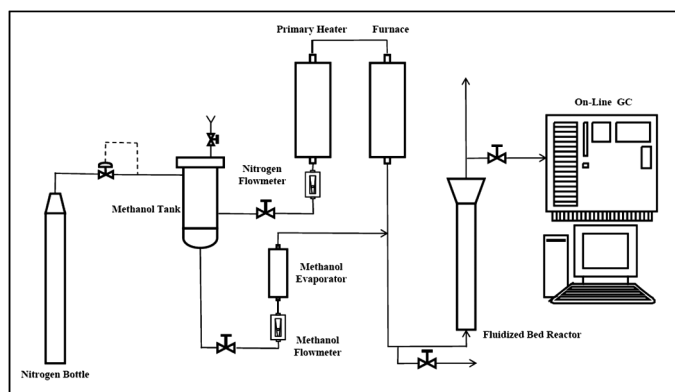14 El-Halwagi, M. M.; El-Rifai, M. A. *Chem. Eng. Sci.* **1988**, *43*, 2477-2486

Fig. 5. Schematic diagram of the experimental set up